Practical Papers, Articles and Application Notes

Robert G. Olsen, Technical Editor

In this issue you will find two practical papers that should interest members of the EMC community. The first is entitled "Estimating Measurement Uncertainty: A Brief Introduction to the Subject," by Ed Bronaugh and Don Heirman. In this paper, the authors provide an introduction to the problem of estimating the uncertainty of measurements conducted in laboratories accredited to ISO/IEC 17025. Portions of the work in this paper have been presented with the permission of the United States EMC Standards Corporation. The second, entitled "Magnetic Light Technology – Illumination for the 21st Century and Beyond" by Steve Vetorino, Geoffrey Wilson and Russell Sibell is a fascinating technical overview of the thought process behind the design of a new technology for flashlights without batteries. This flashlight operates on energy stored in a capacitor that was generated by shaking a very powerful magnet through a coil to magnetically induce a current in an electrical circuit. I think you will find it to be a good example of the thinking behind the design of new products.

The purpose of this section is to disseminate practical information to the EMC community. In some cases the material is entirely original. In others, the material is not new, but has been made either more understandable or accessible to the community. In others, the material has been previously presented at a conference but has been deemed especially worthy of wider dissemination. Readers wishing to share such information with colleagues in the EMC community are encouraged to submit papers or application notes for this section of the Newsletter. See page 3 for my e-mail, FAX and real mail address. While all material will be reviewed prior to acceptance, the criteria are different from those of Transactions papers. Specifically, while it is not necessary that the paper be archival, it is necessary that the paper be useful and of interest to readers of the Newsletter.

Comments from readers concerning these papers are welcome, either as a letter (or e-mail) to the Associate Editor or directly to the authors.

Estimating Measurement Uncertainty A Brief Introduction to the Subject

Edwin L. Bronaugh and Donald N. Heirman

EdB™ EMC Consultants, 10210 Prism Drive, Austin, Texas 78726-1364

ed.bronaugh@ieee.org

Don HEIRMAN Consultants, 143 Jumping Brook Road, Lincroft, New Jersey 07738-1442

d.heirman@ieee.org

Abstract

Whenever an EMC measurement is made, there are numerous uncertainties in different parts of the measurement system and even in the EMC performance of the EUT which is being measured. It is important to be able to estimate the overall uncertainty, in particular, the test setup and measurement equipment uncertainty. Making repetitive measurements can reduce the measurement uncertainty, but often economics of time do not permit that. We discuss methods for estimating the uncertainty of EMC measurements using Normal, Log-normal, rectangular, triangular, and u-shaped distributions. We provide references that the reader can use to learn more about uncertainty of measurements. We discuss how these references apply to specific uncertainty estimating tasks. We provide guidance and explanations for developing an uncertainty budget; finding combined standard uncertainty and expanded uncertainty. We discuss sensitivity coefficients and confidence intervals for the expanded uncertainty and provide calculation and derivation examples.

Introduction

Since the spring of 1992, and particularly in the past five years, there has been a resurgence in the need for understanding and applying the basic principles of measurement uncertainty. In the past two years there has been significant international attention drawn to the need for estimating and applying measurement uncertainty, especially for those laboratories that are accredited to ISO/IEC 17025 [1][1] on the competency of calibration and testing laboratories. ISO/IEC 17025 addresses measurement uncertainty in several clauses that have to be considered during a laboratory assessment. For our EMC discipline, there have been several documents, which we will cite later in this article, which describe how to estimate and use measurement uncertainty in EMC measurements. Most notable is the international standard CISPR 16, Part 4-2 [2]. CISPR is the International Special Committee on Radio Interference. We will briefly describe its contents near the end of this article. But now we will introduce the basic concepts of uncertainty, which should give you a basic understanding in your pursuit of quality EMC measurements.

Uncertainty is a parameter associated with the result of a measurement. It characterizes the dispersion of the values that could be reasonably attributed to the measurand [3] [4]. The measurand is the quantity being measured, not the physical device or equipment under test (EUT). There are several types of uncertainty. The three with which we will work are standard uncertainty, combined standard uncertainty, and expanded uncertainty.

Standard Uncertainty

Standard uncertainty is usually denoted as u_s. It is the uncertainty of the result of a measurement and it is expressed as a standard deviation. Usually it is expressed as the standard deviation (or error) of the mean value of a set of independent measurements using the same instruments. For normal[2] distributions it is as shown in Equation (1).

$$u_s = s(\overline{q}) = \frac{s(q_j)}{\sqrt{n}} \tag{1}$$

where: u_s is the standard uncertainty, $s(\overline{q})$ is the standard deviation of the mean value of a distribution of data (sometimes called the standard error of the mean), $s(q_j)$ is the standard deviation of values of q in the distribution, and n is the number of values of q.

Other expressions are used for non-normal distributions, such as rectangular distributions, triangular distributions, u-shaped distributions, and trapezoidal distributions. The latter one is seldom used in EMC test uncertainty estimates. We will describe these other distributions later in this article.

Combined Standard Uncertainty

The combined standard uncertainty is the uncertainty of a result when it is obtained from the values of several other statistically independent quantities. It results when these independent quantities are combined using the *Law of Propagation of Uncertainty* [3] [4]. These independent quantities are usually the uncertainties associated with the influence quantities, *i.e.*, the errors and deviations from ideal, of the instrumentation used for the measurement. They are combined by root-sum-square (RSS) addition. The combined standard uncertainty is equal to the positive square-root of a sum of terms, which are the weighted variances and covariances of the standard uncertainties of the influence quantities. An example is shown in Equation (2).

$$u_c = \sqrt{c_1^2 u_1^2 + c_2^2 u_2^2 + \cdots + c_n^2 u_n^2} \tag{2}$$

The c_i terms are the sensitivity coefficients of the uncertainties being combined. The sensitivity coefficients arise when an uncertainty has either more or less influence on the result compared to the other quantities. Unless there is evidence to the contrary, the sensitivity coefficients are assumed to be unity. Sensitivity coefficients are discussed in Appendix A. Note that the influence quantities with the largest sensitivity coefficients or the overall largest values, will then be those that contribute the most to uncertainty; and, hence will lead the investigator to those quantities needing to be reduced.

If any of the influence quantities include a bias or systematic effect, effort should be made to separate it from the random part of the error in the quantity before forming the uncertainty.

Expanded Uncertainty

The expanded uncertainty is a quantity defining an interval about the result of a measurement that is expected to encompass a large fraction of the possible values of the result. It approximates a specified probability of containing the true value (coverage) of the measurand. It is based on a coverage factor k, which is usually 2 or 3, but may have other values. A few values of k related to the probability of coverage are tabulated below:

TABLE 1. EXAMPLE COVERAGE FACTORS

Prob., %	50	68.27	80	90	95.45	99.73	99.99
k	0.675	1	1.28	1.645	2	3	3.89

Some of these values are familiar from statistical tables. The probability of coverage is usually mentioned as approximately 68% or approximately 95% (with its respective coverage factors of 1 or 2), *etc*. This sometimes is called a "confidence interval" which is not as precise as "coverage" as identified here.

Bias or Systematic Corrections

Bias or systematic effect is common in EMC measurements. We use correction factors, *e.g.*, cable loss; conversion factors, *e.g.*, antenna factors; and bias in specific instrumentation, *i.e.*, "reads about 2 dB low." Each systematic effect has two elements, a known or approximately known or expected value, μ, and a random variation about the expected value, u_μ. The expected value is used as a direct correction of the measurand, and the random variation is combined into the uncertainty of the measurement. The random variation may be given as a tolerance or error, in which case it has to be converted to an uncertainty by applying a distribution function so that we know how these tolerances are distributed. For example, if a tolerance is ± 2 dB, where in that range is it most likely to occur? A properly chosen distribution function would provide that estimate. When a tolerance is given, *e.g.*, in a manufacturer's technical manual, a rectangular distribution is usually used. We will cover more on that later.

For EMC measurements, decibels are usually used for stating uncertainty estimates if there are no additive effects, *e.g.*, ambient noise **adding** to signals from the EUT. If there are additive effects, the affected data are first converted, if necessary, to linear values, then the necessary addition or subtraction is performed, and finally the result is converted back to decibels.

Documents for Measurement Uncertainty

The following documents are used as references and a bibliography for measurement uncertainty. These are listed in full at the end of this article in the "References" section.

The first document is *ISO Guide to the Expression of Uncertainty in Measurements*. It was first published in 1993 and then corrected and republished in 1995. It is the basis of *all* measurement uncertainty use and estimates worldwide. It was developed jointly by the following international standards committees: BIPM, IEC, IFCC, ISO, IUPAC, IUPAP, and OIML. It is usually referred to simply as *The Guide* or sometimes as *The GUM*. [3] These standards committees are: BIPM, Bureau international des poids et measures; IEC, International Electrotechnical Commission; IFCC, International Federation of Clinical Chemistry; ISO, International Organization for Standardization; IUPAC, International Union of Pure and Applied Chemistry; IUPAP, International Union of Pure and Applied Physics; and, OIML, International Organization of Legal Metrology.

The second document is ANSI/NCSL Z540-2, *American National Standard for Expressing Uncertainty—U.S. Guide to the Expression of Uncertainty in Measurement*. It was published in 1997. It contains exactly the same information as *The Guide*, but is written in US English rather than Oxford English, which for example deprecates the use of "z" in such words as "standardization" where the "z" is replaced by an "s". [4]

The third document is NIST TN 1297, *Guidelines for Evaluating and Expressing the Uncertainty of NIST Measurement Results*. It was published in 1994. It is the NIST interpretation and application of *The Guide* to NIST activities. It applies generally to laboratory measurements (not specifically to EMC measurements) and is easier to read than *The Guide*. [8]

The fourth document is CISPR 16, "*Specification for radio disturbance and immunity measuring apparatus and methods: Part 4-2: Uncertainties, statistics and limit modeling: Uncertainty in EMC measurements.*" This standard was the first international standard on EMC measurement uncertainty. It provides examples of how to calculate the uncertainty estimates for radiated and conducted emissions and emission power (absorbing clamp) measurements. In addition, it specifically provides target measurement instrumentation uncertainty values for the three measurements just cited and indicates how a testing laboratory shall use its own values in accounting for its measurement instrumentation uncertainties in determining whether a product passes or fails any of three measurement emission limits. [2] Note that CISPR 16-4-2 is a recent reorganized document which contains the uncertainty information in the former CISPR 16-4.

The fifth document is UKAS LAB 34, *The Expression of Uncertainty in EMC Testing*. It was published in 2002 and applies specifically to EMC Measurements. The UKAS Executive, National Physical Laboratory, in the United Kingdom, developed it. It is UKAS' interpretation of *The Guide*, and applies specifically to laboratories that are accredited by UKAS. UKAS is the United Kingdom Accreditation Service. [9]

The sixth document is also a UKAS document, M3003, *The Expression of Uncertainty and Confidence in Measurement*. It was published in 1997 and is a rewrite of an earlier document called NIS 3003. It is a useful reference because it goes deeper than NIST TN 1297, but not so deep as *The Guide* or ANSI/NCSL Z540-2. [10]

The seventh document is a book, *The Lognormal Distribution*, by J. Aitchison and J. A. C. Brown. Cambridge University Press in England published it in 1957. The Lognormal distribution was developed in the late 1800s to analyze *multiplicative* data. (The Normal or Gaussian distribution was designed much earlier to analyze *additive* data.) The Lognormal distribution gives the proper method of analyzing data such as correction factors and conversion factors, which are multiplicative. It allows EMC test data and instrumentation data to be converted to decibels (dB) and then used with the Normal distribution for statistical analysis. [5] Additive data are combined or manipulated using addition and subtraction, while multiplicative data are combined or manipulated using multiplication and division. The name "factor" immediately implies that the quantity is multiplicative.

The eighth document is an EMC symposium paper, "Estimating EMC Measurement Uncertainty Using Logarithmic Terms (dB)," written by E. L. Bronaugh and J. D. M. Osburn and presented at the *1999 IEEE International Symposium on Electromagnetic Compatibility* in Seattle, WA. [11]

The ninth document is an EMC Transactions paper, "*CISPR Subcommittee A Uncertainty Activity,*" written by D. N. Heirman and published in the *IEEE Transactions on EMC,* Vol. 44, No. 1, February 2002. [7]

The tenth document is an EMC Symposium paper, "A Demystification of the U-Shaped Probability Distribution," written by Darren Carpenter and presented in the *2003 IEEE Symposium on Electromagnetic Compatibility* in Boston, MA. [6]

The eleventh document is a book, *The Uncertainty of Measurements, Physical and Chemical Metrology: Impact and Analysis*, by S. K. Kimothi, published in 2002 by American Society for Quality. It is a good and thorough textbook on estimating uncertainty. [12]

The twelfth document is ISO/IEC 17025, *General Requirements for the Competence of Calibration and Testing Laboratories*. Published in 1999. [1]

ISO Guide Approach

According to the basic resource documents [3] [4] for measurement uncertainty, a statement of expanded uncertainty (U) shall accompany every measurement. The expanded uncertainty has a specified probability of containing the true value, *i.e.*, a probability of coverage (sometimes called a "confidence interval"). If the true value is Y, the measured value is y, and the uncertainty of the measurement is U, then $Y = y \pm U$. That is, Y lies within the range from $y - U$ to $y + U$. The expanded uncertainty was already defined in the introduction.

There are two types of evaluations of uncertainty, Type A and Type B. Type A evaluation is the method of evaluation of uncertainty by the statistical analysis of a series of n observations of an influence quantity or of the measurand using the same instruments. Type B evaluations include all other methods. Type B evaluations may be based on:

- Previous measurement data;
- Data provided in calibration and other certificates (without descriptive statistics);
- Manufacturer's specifications, *e.g.*, tolerances;
- Experience with, or general knowledge of, the properties of instruments and materials; and,
- Uncertainties assigned to reference data taken from handbooks.

Distributions Used in Type A Evaluations

The probability distributions used in Type A evaluations are the Normal distribution and the Lognormal distribution. The Normal (sometimes called Gaussian) distribution is designed for analyzing additive data, and the Lognormal distribution is designed for analyzing multiplicative data. Note that for most EMC measurements, which are logarithm based, the Lognormal distribution applies, because the value being measured is multiplied or divided by the correction and conversion factors associated with the instrumentation.

The Normal distribution is applicable only to additive data, and has the typical "bell curve" found by descriptive statistics, student's-t analysis, or other statistical approaches. It is assigned to standard uncertainty, combined standard uncertainty, and expanded uncertainty. The common formulae for the Normal distribution are shown in Equations (3), (4), and (5) below. As noted above in Equation (1), but for emphasis, repeated here:

$$u_s = s(\overline{q}) \tag{3}$$

u_s is the standard uncertainty and $s(\overline{q})$ is the standard deviation (or error) of the mean value.

$$s(\overline{q}) = \frac{s(q_j)}{\sqrt{n}} \tag{4}$$

$s(q_j)$ is the standard deviation of the distribution of values of q, and n is the number of values in the distribution. This is shown below in Equation (5).

$$s(q_j) = \sqrt{\frac{1}{n-1}\sum_{j=1}^{n}(q_j - \overline{q})^2} \tag{5}$$

and n is the number of repeated measurements.

Equation (5) gives the sample standard deviation, and Equation (4) gives the standard deviation or error of the mean value, and the mean value is shown in Equation (6). Equation (3) shows that the standard uncertainty is equal to the standard deviation of the mean. The Normal distribution is shown in Figure 1. As in all probability distributions, the area under the curve is equal to 1. In Figure 1, the vertical dashed lines show the mean and the first standard deviations above and below it.

$$\overline{q} = \frac{1}{n}\sum_{j=1}^{n} q_j \tag{6}$$

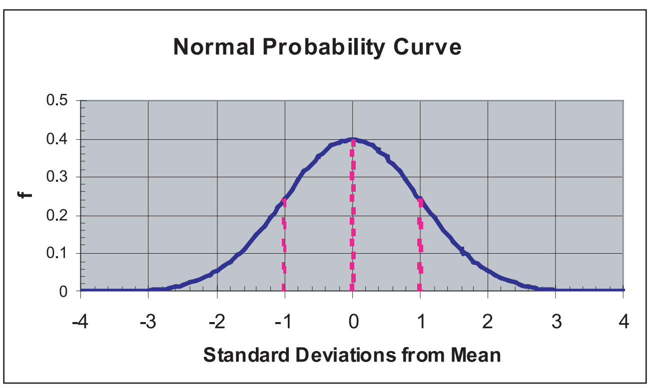

Figure 1. Normal (Gaussian) Distribution

Note that percentages are not additive except in the special case where they all have the same base. The base is the number which is multiplied by the percent to get the percentage. For example, if the quantity or base is 45, then 10% of it is 4.5, 5% of it is 2.25, 30% of it is 13.5, *etc.* These are all additive because they represent fractions of 45. However, if one percentage is 5% of 45 and another is 10% of 70, these percentages (4.5 and 7) are not additive because they represent fractions of different numbers or bases.

The Lognormal distribution is applicable only to multiplicative data (the term multiplicative includes both multiplication and division). Its mean value is the geometric mean, shown in Equation (7). The Lognormal distribution was developed in the late 1800s to analyze log normally distributed (multiplicative) data [5]. The Lognormal distribution has no zero or negative values. Its transform, Equation (8), converts multiplicative data to additive data that can then be used with the Normal distribution.

$$\overline{X}_{LN} = \sqrt[n]{\prod_{j=1}^{n} x_j} \tag{7}$$

$$Y = \text{Ln}\,X \tag{8}$$

Multiplicative data of the type used in EMC measurements are log normally distributed. EMC data correction factors and conversion factors are all positive when stated in linear terms. For example, the correction factor for cable loss can be stated in linear terms (or in decibels), *e.g.*, a division by 1.189 (or 1.5 dB loss), or a multiplication by 0.841 (or a –1.5 dB gain). The Lognormal distribution is shown in Figure 2 and its transform is shown in Figure 3 [5]. Again, the area under the curve is 1.

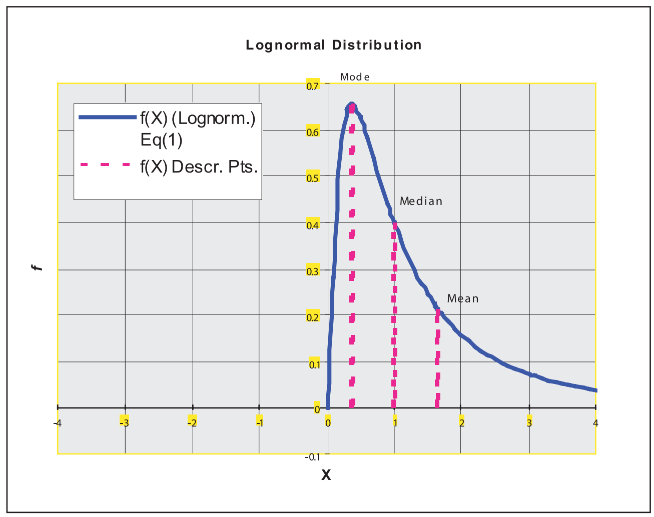

Figure 2. The Lognormal Distribution

Notice that the peak of the Lognormal distribution is the Mode, the Mean is the geometric mean, given by Equation (7), and the Median is half-way between the Mode and the Mean. The term “Descr. Pts.” in Figures 2 and 3 means “descriptive points,” *i.e.*, median, mode, mean, *etc.*

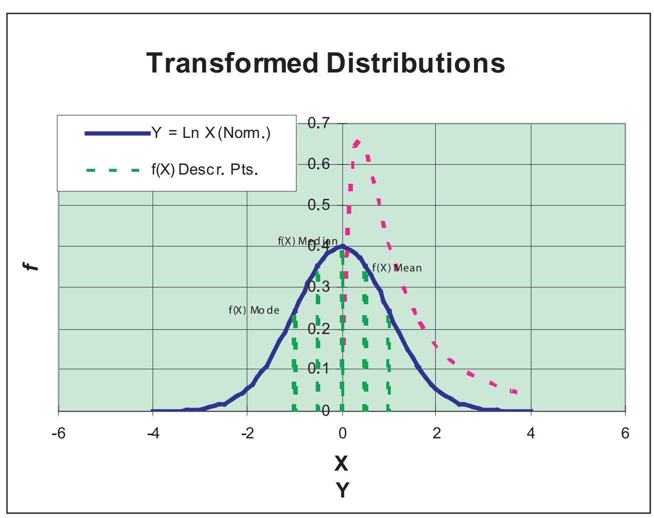

Figure 3. The Transform of the Lognormal Distribution

The importance of the Lognormal distribution is this: It shows that it is correct to use logarithmic terms, *i.e.*, decibels for statistical analysis of EMC data. It is shown in detail here to emphasize its utility in EMC measurement uncertainty analysis.

The transformation from Lognormal to Normal is via Equation (8). Both X and Y are data values on the horizontal axis. As in the Lognormal distribution, the vertical axis shows the frequency of occurrence of the data values. Note where the Mean, Median, and Mode values of the Lognormal distribution appear after the transformation. The Lognormal Median has become the Mean of the transformed data, and the Lognormal Mode has become approximately the Standard Deviation of the transformed data. For comparison, the Lognormal distribution is shown as a dashed pink curve in Figure 3.

Distributions Used in Type B Evaluations

The three most important distributions used in Type B evaluations are the rectangular distribution, the a-priori (triangular) distribution and the u-shaped distribution.

- The rectangular distribution is used where all values in a continuum are equally likely. For example, if a tolerance is stated as ± 3 dB and you have no other information, there is equal likelihood that any value within the range between -3 dB and $+3$ dB exists, thus a rectangular distribution function applies. A manufacturer's specified tolerance or error is a typical example.
- The a-priori distribution is used where the analyst has prior knowledge, or has good reason to suspect, that the values tend to be clustered near the center of a continuum. In the example above, that would be close to 0 dB. For example, the uncertainty associated with site attenuation measurements could be estimated using the a-priori distribution function as it is more likely that the deviations from theoretical site attenuation cluster closer to 0 dB than ± 4 dB for a good test site.
- The u-shaped distribution is used where the values tend to be clustered near the ends of a continuum or in fact become infinite at the ends of the continuum. An example is the effect of VSWR between two instruments in the measurement instrument chain.

These distributions are used to put Type A and Type B evaluations on the same "footing." Their equivalent descriptive statistics may be estimated from calculations using statistically sound approximations. They allow combining, with appropriate weights, uncertainties from various sources via the law of propagation of uncertainty. The resulting combined standard uncertainty is considered normally distributed. The expanded uncertainty can thus maintain its prediction of coverage probability.

Weights or Weighting Factors. Depending on the distribution used, the errors or tolerances have different effects on the resulting uncertainties. These weighting factors are not "sensitivity coefficients," but instead tell us how much weight the error or tolerance has for a particular distribution.

Rectangular Distribution. In the rectangular distribution the true value X_i may, with equal probability, lie anywhere in the interval a_+ to a_-. From mathematical analysis (see Appendix B), for symmetrical data, $u_s = a/\sqrt{3}$. The weighting factor is $1/\sqrt{3}$. If the data are unsymmetrical, understand why and/or

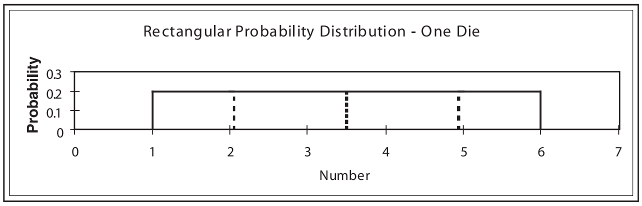

Figure 4. Rectangular Probability Distribution Example Using the Probability of One Fair Die

be prepared to do further analysis. In estimating measurement uncertainty, this distribution is applied to such things as manufacturer-specified tolerance or error, or any other influence quantity in which all values in a continuum are equally likely. Figure 4 shows an example of a Rectangular distribution. This example uses a discrete random variable that has only integer values from 1 to 6. However, it serves to illustrate the application of the rectangular distribution for continuous random variables as well. This distribution is that of a six-sided cube with one of the numbers 1 – 6 on each face, *i.e.*, a die used in games. $a = (6 - 1)/2 = 2.5$, thus $u = 2.5/\sqrt{3} = 1.44$. The Mean is at $1 + 2.5 = 3.5$ and the uncertainties (standard deviations) are at $3.5 - 1.44 = 2.06$ and $3.5 + 1.44 = 4.94$.

Triangular (*A-Priori*) Distribution. In this distribution the true value X_i lies in an area near the center of the interval from a_+ to a_-. From mathematical analysis, $u_s^2 = a^2/6$, and $u_s = a/\sqrt{6}$. The weighting factor is $1/\sqrt{6}$. In estimating EMC measurement uncertainty, the *a-priori* distribution would be applied to processes known to produce tightly clustered centrally located data, for example, site attenuation deviation from theoretical values on a well-behaved Open-Area Test Site. Figure 5 shows an example of a Triangular distribution. It is called *a-priori* because the analyst needs prior knowledge of the process to which it is applied. That is, some reason has to be known in advance of making a measurement that the data tend to be clustered near the center of the distribution. Again, a discrete random variable is used to illustrate the properties of the distribution.

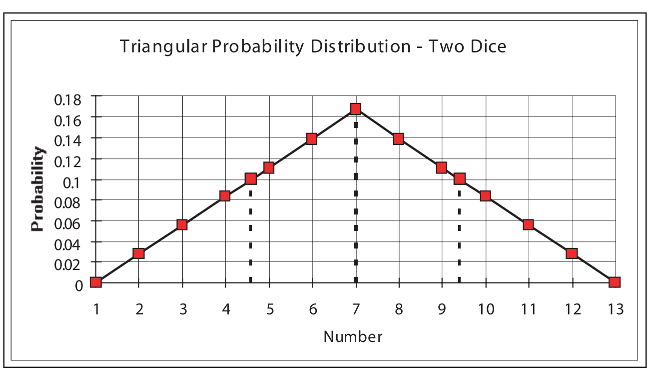

Figure 5. Triangular Probability Distribution Using the Probability of Two Fair Dice

U-Shaped Distribution. This distribution is applied to the analysis of the results of combining two vector quantities, such as the vector addition of two electromagnetic fields impinging on an antenna, or the results of combining forward and reflected signals in a cable between two devices connected to it when neither device matches the impedance of the cable. This is a common problem in EMC measurements. The effect of VSWR on measurement uncertainty is described by a u-shaped distribution.

A u-shaped distribution is shown in Figure 6. The true value X_i is concentrated near the ends of the interval a_+ *to* a_- and from mathematical analysis, $u_s^2 = a^2/2$, and the uncertainty is $u_s = a/\sqrt{2}$. The weighting factor is $1/\sqrt{2}$. When applying the u-shaped distribution to find the uncertainty caused by VSWR, the following formulae are used, where a is replaced by M, and M is the mismatch error. This can be done in decibels or percent, although the use of percent in uncertainty is deprecated except when the percentages all have the same base.[3]

$$M = 20\lg(1 \pm |\Gamma_1||\Gamma_2|), \text{dB} \tag{9}$$

or

$$M = 100\left[(1 \pm |\Gamma_1||\Gamma_2|)^2 - 1\right], \% \tag{10}$$

and

$$u(x_i) = \frac{M}{\sqrt{2}}, \text{dB (or \%)} \tag{11}$$

Note that the two limits of M found when using either Equation (9) or Equation (10) are asymmetric around the result of the measurements, but the difference this makes to the total uncertainty is usually insignificant. When using Equation (9)—preferred—it is acceptable to use the larger of the two limits, *i.e.*, $20\lg(1 - |\Gamma_1||\Gamma_2|)$. Γ_1 and Γ_2 are the reflection coefficients of the mismatch at the ends of the cable.

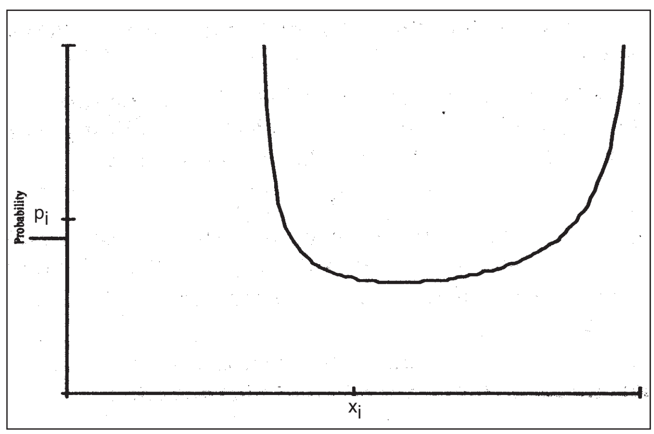

Figure 6. The U-Shaped Probability Distribution [6]

Figure 6 shows that the u-shaped distribution is not symmetrical. The figure was machine drawn from Equations (12) and (13). These Equations, from [6] are: first, Equation (12) for the combined voltage at position x_i along the cable,

$$V_C(x_i) = \sqrt{V_1^2 + V_2^2 + 2V_1V_2\cos\theta} \tag{12}$$

where V_1 is the incident voltage, V_2 is the reflected voltage, and θ is the phase difference between the two waves; and, second, Equation (13) for the probability of the combined voltage,

$$P(V_C) = \frac{2V_C}{\pi\sqrt{(V_{\max}+V_C)(V_{\max}-V_C)(V_C+V_{\min})(V_C-V_{\min})}} \tag{13}$$

where $V_{\max} = V_1 + V_2$, and $V_{\min} = V_1 - V_2$.

Note that there will be two points at which the denominator of (13) becomes zero.

Combining Rectangular Distributions. This discussion may help one understand why the combined standard uncertainty is considered to be normally distributed. The example shown in Figure 5, a triangular (*a-priori*) distribution, is the result of combining two rectangular distributions. It is for two fair dice rolled at the same time. There are possible outcomes from 2 through 12. Note that the probability of rolling 1 or 13 is zero, and that the highest probability is rolling a 7, which is the mean value of the distribution. The two dashed verticals, one either side of the mean are the two standard deviations (uncertainties) subtracted from 7 or added to 7, *i.e.*, 4.6 and 9.6. When a third rectangular distribution is added, the result begins to look much like a Normal distribution, and the more rectangular distributions that are added, the more the resulting distribution approaches a Normal distribution.

Establishing Uncertainty Budget

The issues to be considered follow.

The Range of Measurements. Break down the range, *e.g.*, by: frequency, test specification, test equipment, and/or limits.

List the Influence Quantities. For example: test and measurement instrumentation, test site, EUT, and other influences.

Type A Evaluation applies to random variations while measurements are being made and repeated under the same conditions. Use Equations (3), (4), and (5). Use Equation (6) to find the mean value of the measurements. Repeated measurements are especially needed when measured results are close to the specification limit. Use the typical test process and configuration. For example, an OATS repeat radiated emission measurement may include connecting and reconnecting antenna and cable and receiver, and remaximizing the received signal by varying antenna height and turntable position. Such "n" repeated measurements will reduce the measurement uncertainty by the "$\sqrt{n}$". This of course will require more test time and care which may or may not be practical. Yet if the measurement uncertainty needs to be lowered, this is an excellent way to lower it, and provide the most realistic measurement uncertainty.

Note that the term is "repeatability" NOT "reproducibility." Repeatability occurs at the same laboratory with the same instrumentation and the same test operator. Reproducibility occurs when the same EUT is tested at two, or more, laboratories, different instrumentation is used, or different operators do the tests. See the definitions in [3] or [4].

Type B Evaluation applies to all other significant contributions to uncertainty. A Type B quantity (*e.g.*, receiver accuracy) remains constant during measurements if instrument settings are constant, but it may change if measurement conditions change (*e.g.*, change of receiver attenuator setting). One should use a Type B evaluation rather than recalibrate test instrumentation, *e.g.*, do not recalibrate the receiver but use a rectangular distribution based on the manufacturer's specifications instead. In order for recalibration of an instrument to be more effective than using the manufacturer's specifications in a Type B evaluation, the instrument would need a Type A evaluation using repeated calibration against a stable standard having low uncertainty.

Uncertainty Distributions. Most distributions are symmetrical, *e.g.*, receiver amplitude uncertainty. However, some are asymmetrical such as different uncertainties for positive phase addition of signals than for negative phase addition, *e.g.*, effects of VSWR.

Combining Uncertainties of Influence Quantities. Use Equation (2), *i.e.*, RSS, for independent uncertainties. For errors that are not independent, *e.g.*, signal plus noise, first use arithmetic addition (subtraction) to correct the signal level for the noise, then convert the resulting signal level to decibels and put this into the RSS to find the combined standard uncertainty.

Expanded Uncertainty. Use standard confidence levels employing a coverage factor k. Use $k = 2$ for $\approx$95% confidence, in most tests. The coverage factor k may have to be greater than 2 to provide 95% confidence if the uncertainty is derived from a small sampling of repeated measurements.

Reporting Results. The strict use of the GUM [3] [4] indicates that the reporting of the measured data shall be the actual measurement result $\pm$ expanded uncertainty and the value of k used for expansion. Expanded uncertainty is usually designated by "U." Note that later in this article we will discuss the CISPR 16-4 approach which does not add the full expanded uncertainty for the three emission tests discussed.

Example. In a conducted emission measurement, the test setup may be as shown in Figure 7, and the uncertainty budget as shown in Table 2. This example shows what contributors might typically be included, but is not all-inclusive.

WARNING: The values used in this example are fictitious—they are just for example and should not be simply taken on board for calculation of any individual uncertainty estimate for your instrumentation chain!

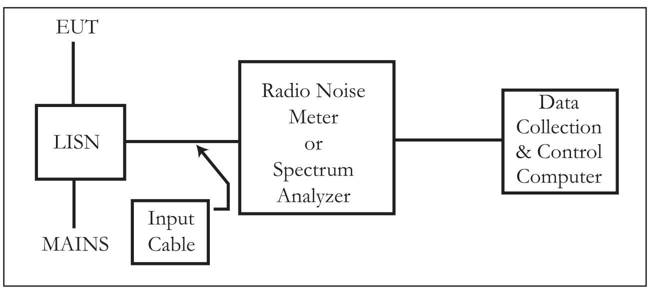

Figure 7. Conducted Emission Test Setup Example

The LISN (Line impedance stabilization network, also called an artificial mains network abbreviated AMN), input cable, and receiver (radio noise meter) are analyzed in Table 2.

Notice that the influence quantities for the cable and input attenuator calibration, the mismatch tolerance, and the system repeatability (rows 3, 4 and 5) are different in the two frequency ranges chosen. The two frequency ranges were chosen specifically for this reason. The worst-case values could be used throughout the entire frequency range, but it makes sense to split the frequency range so that the resulting uncertainties will be more realistic.

The first two quantities (rows) in Table 2 are manufacturer's gain (or loss) tolerances for which a rectangular distribution is used. In Equation (14) they are divided by 3, the square of the weighting factor. The third quantity is from calibration data and is expanded uncertainty so it is divided by the k-factor. The fourth quantity is mismatch effect. It is calculated from the worst-case values of reflection coefficients using Equation (9). The fifth quantity is the variability of repeated measurements of the EUT (with only one reading of the EUT, *i.e.*, measured at only one frequency). Ten repeats are made, that is, $n = 10$. The standard deviation of the mean is used, *i.e.*, Equations (3) and (4). Since it is a standard deviation, $k = 1$.

The sixth quantity is basically a placeholder. If several EUTs had been evaluated, this influence quantity would have resulted in an estimate of the probability that any EUT of the same type and manufacturer would always produce the same emission level. It is not usually cost-effective to thoroughly test several EUTs, thus this influence quantity is usually ignored. However, when several units are tested in an 80%–80% analysis, the data collected can be used to form the basis of this sixth influence quantity. The combined standard uncertainty is found by Equation (2) and it is multiplied by $k = 2$ to find the expanded uncertainty U.

The example calculations by frequency range are shown below. The combined standard uncertainty is denoted by u_c. Note that the weighting factors and k-factors of the influence quantities are used as divisors in Equations (14) and (16). The sensitivity coefficients are all unity.

<u>9 – 150 kHz:</u>

$$u_c = \sqrt{\left(\frac{1.5^2 + 1.5^2}{3}\right) + \left(\frac{0.3}{2}\right)^2 + \frac{0.2^2}{2} + 0.2^2} = 1.26 \text{ dB} \tag{14}$$

$$U = 2 \times 1.26 = 2.5 \text{ dB} \tag{15}$$

<u>0.15 – 30 MHz:</u>

$$u_c = \sqrt{\left(\frac{1.5^2 + 1.5^2}{3}\right) + \left(\frac{0.5}{2}\right)^2 + \frac{0.05^2}{2} + 0.35^2} = 1.30 \text{ dB} \tag{16}$$

$$U = 2 \times 1.30 = 2.6 \text{ dB} \tag{17}$$

A simple test that may be used to discover if the k-factor should be larger than 2 to assure 95% confidence that the true value lies within the range $y - U \leq Y \leq y + U$ is shown in Equation (18). When this inequality is true, $k = 2$ will assure 95% confidence.

$$\frac{u_c}{u_5} \geq 3 \tag{18}$$

where u_5 is the standard uncertainty of the fifth influence quantity (the repeatability test) in Table 2.

In this example u_5 is 0.2 dB below 150 kHz and 0.35 dB above 150 kHz. In this example,

$$\frac{1.26}{0.2} = 6.3 > 3, \quad \text{and} \quad \frac{1.30}{0.35} = 3.7 > 3 \tag{19}$$

showing that $k = 2$ is large enough to assure 95% confidence. See Appendix C for an explanation of this check method (often referred to as "degrees of freedom").

CISPR Uncertainty

CISPR in its publication CISPR 16-4-2[2] has addressed specific application of EMC measurement instrumentation uncertainty. This was the culmination of close to seven years of study

TABLE 2. CONDUCTED EMISSION EXAMPLE

Influence Quantity	*Distribution*	*Tolerance or Uncertainty, dB 9–150 kHz*	*Tolerance or Uncertainty, dB 0.150–30 MHz*
Receiver Specification (Tolerance)	Rect.	±1.5	±1.5
LISN Coupling Spec. (Tolerance)	Rect.	±1.5	±1.5
Cable & Input Attenuator Calibration (Expanded $U(k = 2)$)	Norm.	±0.3	±0.5
Mismatch Tolerance: Rcvr. $\Gamma_R = 0.03$ LISN $\Gamma_L = 0.8$ (9 kHz) 0.2 (30 MHz)	U-shaped	±0.2	±0.05
System Repeatability $s(q_k)$, $n = 10$ (1 reading on EUT)	Std. Dev.	±0.2	±0.35
Repeatability of EUT	—	—	—
Combined Std Uncertainty	Norm.	±1.26	±1.30
Expanded Uncertainty $U(k = 2)$	Norm.	±2.5	±2.6

in CISPR Subcommittee A. As might be imagined, this concept was not immediately met with acceptance as there was no experience in estimating EMC measurement uncertainty. In addition, there were issues of what should be included in an EMC measurement uncertainty. At the end, the subcommittee decided to initially consider the emission measurement instrumentation uncertainty and its effect on the measured result. This left out uncertainty in, for example, the test setup, EUT emission stability, etc. Reference [7] gives much more detail on the history leading up to the publication of CISPR 16-4-2.

In any case, the basic approach used in CISPR 16-4-2 is to set a target value of measurement instrumentation uncertainty for three emission measurements: radiated, conducted and power. This target value represents a value, which can readily be achieved with careful instrumentation calibration and application. The idea is that if such care is achieved, then the test laboratory need not add any uncertainty to its measured value. If the test laboratory measurement instrumentation uncertainty is greater than the target uncertainty set by CISPR in CISPR 16-4-2, then there has to be a penalty paid by an addition of a value to the measured value. Note that this approach is different than that usually employed by, for example, calibration laboratories, where the measured value always has added to it the range of uncertainty that the calibration instrumentation has. It was agreed by the National Committees of CISPR Subcommittee A that a less severe approach be first considered so as not to penalize those test labs where their uncertainty is equal to or less than the target uncertainty representing a value readily achieved by good calibration and instrumentation use practices.

Table 3 shows the target values set by CISPR 16-4-2 for measurement instrumentation uncertainty for the three tests indicated.

The above table is used in the following manner. If the measurement instrumentation uncertainty of the testing laboratory is less than or equal to the values in Table 3, the measured result is compared to the limit to determine product compliance without taking into account any measurement uncertainty value. If, however, the test laboratory uncertainty is greater than the values in Table 3 above, then the difference between the test laboratory value and the respective Table 3 value for the test in question is added to the measured results and that sum compared to the limit to determine if a product passes or fails.

TABLE 3. TARGET MEASUREMENT INSTRUMENTATION UNCERTAINTY VALUES

Disturbance (emission)	*Frequency Range*	*U_{cispr} (dB)*
Conducted	9 to 150 kHz	4.0
	150 kHz to 30 MHz	3.6
Radiated	30 to 1000 MHz	5.2
Power	30 to 300 MHz	4.5

Finally, there is now additional work that was published in CISPR including a primer on measurement uncertainty taking into account not only the measurement instrumentation uncertainty but also other variables including the test specification as it adds to the uncertainty in, for example, the way in which the test setup is not fully described. This work is included in CISPR 16-4-1 which contains information including basic considerations on uncertainties in emission measurements and immunity testing. [2]

Summary

The work on measurement uncertainty continues for the EMC testing world as well as in international standardization. We do not have space to also review the standardization work in ANSI ASC C63 where there is now a draft guide for estimating EMC measurement uncertainty out for comment. This work is meant to apply in using most of the C63 measurement standards in particular and uses the basic principles noted in this paper and cited references.

This paper has presented the basic tenets of measurement uncertainty estimation. We have shown examples of application specifically to EMC measurement as well as a review of publications and standards that apply and can serve as the references you need to estimate your own test laboratory uncertainty. We hope that this will be useful during laboratory competency assessment as well as for simply improving the quality of EMC measurements in general.

References

[1] ISO/IEC Standard 17025, *General Requirements for the Competence of Calibration and Testing Laboratories*, International Organization for Standards, Geneva, and International Electrotechnical Commission, Geneva, Dec. 1999.

[2] IEC CISPR 16, *Specification for Radio Disturbance and Immunity Measuring Apparatus and Methods*—Part 4-1: *Uncertainties, Statistics and Limit Modeling—Uncertainties in Standardized EMC Tests* and Part 4-2 *Uncertainties, Statistics and Limit Modeling—Uncertainty in EMC Measurements,* International Electrotechnical Commission, Geneva, 2003.

[3] ISO, *Guide to the Expression of Uncertainty in Measurements*, 1993 (corrected and republished in 1995), International Organization for Standards, Geneva.

[4] ANSI/NCSL Z540-2-1997, *American National Standard for Expressing Uncertainty—U.S. Guide to the Expression of Uncertainty in Measurement*, National Conference of Standards Laboratories, Boulder, CO, 1997.

[5] J. Aitchison and J.A.C. Brown, *The Lognormal Distribution.* England: Cambridge University Press, 1957.

[6] Darren Carpenter, "A Demystification of the U-Shaped Probability Distribution," *2003 IEEE Symposium on Electromagnetic Compatibility Record*, 03CH37446, Boston, MA, Aug. 18–22, 2003, pp. 521–525.

[7] D.N. Heirman, "CISPR Subcommittee A Uncertainty Activity," *IEEE Transactions on EMC*, Vol. 44, No. 1, Feb. 2002.

[8] NIST Technical Note 1297, *Guidelines for Evaluating and Expressing the Uncertainty of NIST Measurement Results*, Barry N. Taylor and Chris E. Kuyatt, National Institute of Standards and Technology, Gaithersburg, MD, 1994.

[9] UKAS LAB 34, *The Expression of Uncertainty in EMC Testing*, United Kingdom Accreditation Service, Feltham, Middlesex, UK, 2002.

[10] UKAS M3003, *The Expression of Uncertainty and Confidence in Measurement*, United Kingdom Accreditation Service, Feltham, Middlesex, UK, 1997.

[11] E.L. Bronaugh and J.D.M. Osburn, "Estimating EMC Measurement Uncertainty Using Logarithmic Terms (dB)," *1999 IEEE International Symposium on Electromagnetic Compatibility Record*, Seattle, WA, 1999.

[12] S.K. Kimothi, *The Uncertainty of Measurements, Physical and Chemical Metrology: Impact and Analysis*, Milwaukee, Wisconsin: American Society for Quality, 2002.

Appendix A

Sensitivity Coefficients

Sensitivity coefficients give more or less weight to an uncertainty that has more or less influence on the combined standard uncertainty. Following is a simple example to show one of the origins of sensitivity coefficients and their use. These coefficients may arise from many causes, including experimental "determination" of how sensitive the measurement uncertainty may be to a particular influence quantity, or how strongly a particular influence quantity affects the uncertainty. If an influence quantity has a square law effect on the combined standard uncertainty, it should be included in the RSS with $c_i = 2$.

Example

The voltage across a resistor carrying current is measured with the intent to determine the power being dissipated in the resistor. By Ohm's law,

$$P = \frac{V^2}{R}. \tag{A1}$$

Using Fractional Errors

Taking the partial derivatives of P with respect to V and R in Equation (A1):

$$\frac{\partial P}{\partial V} = \frac{2V}{R} \text{ and } \frac{\partial P}{\partial R} = -\frac{V^2}{R^2} \tag{A2}$$

Given a function $w = f(x, y)$, then the complete differential of the function is:

$$dw = \frac{\partial w}{\partial x}dx + \frac{\partial w}{\partial y}dy \tag{A3}$$

Then, from Eq (A2) & Eq (A3) the differential of power in the Ohm's Law Equation is:

$$dP = \frac{\partial P}{\partial V}dV + \frac{\partial P}{\partial R}dR \tag{A4}$$

The fractional error in the power is the differential of power divided by the power, so both sides of the Equation are divided by power. The left side by P and the right side by V^2/R, resulting in:

$$\frac{dP}{P} = 2\frac{dV}{V} - \frac{dR}{R} \text{ or errors,}$$
$$\varepsilon_{\mathrm{P}} = c_i\varepsilon_V - \varepsilon_R, \text{ where } c_i = 2. \tag{A5}$$

The sensitivity coefficient of the voltage error is 2, because voltage appeared squared in the original Equation (A1). This makes the error in power twice as sensitive to the error in voltage as it is to the error in resistance. The sensitivity coefficient of the resistance error is not shown because it is unity.

Using Logarithmic Errors

Putting Equation (A1) in logarithmic form, in particular, in decibels gives:

$$10\lg P = 20\lg V - 10\lg R, \text{ dB} \tag{A6}$$

If P has an error ΔP that is small compared to P, caused by similarly small errors in V and R, then:

$$10\lg(P + \Delta P) = 20\lg(V + \Delta V) - 10\lg(R + \Delta R), \text{ dB} \tag{A7}$$

The errors, ΔP, ΔE, and ΔR may be positive or negative. To find the error in P with respect to the errors in V and R, subtract 10 lg P from both sides, that is:

$$10\lg(P + \Delta P) - 10\lg P = 20\lg(V + \Delta V) - 20\lg V$$
$$- [10\lg(R + \Delta R) - 10\lg R], \text{ dB} \tag{A8}$$

Which becomes:

$$10\lg\left(\frac{P + \Delta P}{P}\right) = 20\lg\left(\frac{V + \Delta V}{V}\right)$$
$$- 10\lg\left(\frac{R + \Delta R}{R}\right), \text{ dB} \tag{A9}$$

Which reduces to:

$$10\lg\left(1+\frac{\Delta P}{P}\right) = 20\lg\left(1+\frac{\Delta V}{V}\right) - 10\lg\left(1+\frac{\Delta R}{R}\right), \text{dB} \quad \text{(A10)}$$

Or, in terms of the errors from Equation (A5):

$$10\lg(1+\varepsilon_P) = 20\lg(1+\varepsilon_V) - 10\lg(1+\varepsilon_R), \text{dB} \quad \text{(A11)}$$

This gives errors in terms of dB as:

$$\varepsilon_{P_{dB}} = 10\lg(1+\varepsilon_P),\ \varepsilon_{V_{dB}} = 20\lg(1+\varepsilon_V), \text{ and} \quad \varepsilon_{R_{dB}} = 10\lg(1+\varepsilon_R) \quad \text{(A12)}$$

Note that the sensitivity coefficient $c_i = 2$ is now contained in the decibel form for V, *i.e.*, $10\lg V^2 = 20\lg V$.

See Appendix B of M3003 [10] for more discussion of how sensitivity coefficients arise.

Appendix B

Uncertainty of the Rectangular Distribution

Given a rectangular distribution of which the midpoint is x_i and the limits are $x_i \pm a$, the area of the distribution must be 1 (*i.e.*, 100% probability); therefore, the height of the rectangle must be $1/(2a)$.

The variance is thus:

$$u_{x_i}^2 = \int_{-a}^{a} x^2 P dx \quad \text{(B1)}$$

Substitute P, then:

$$u_{x_i}^2 = \int_{-a}^{a} \frac{x^2 dx}{2a} = \left[\frac{x^3}{6a}\right]_{-a}^{a} \quad \text{(B2)}$$

$$u_{x_i}^2 = \left(\frac{a^3}{6a}\right) - \left(\frac{-a^3}{6a}\right) = \frac{a^2}{3} \quad \text{(B3)}$$

Therefore, the standard uncertainty is:

$$u_s = u_{x_i} = \frac{a}{\sqrt{3}} \quad \text{(B4)}$$

Appendix C

Degrees of Freedom

When an influence quantity is developed from a normal distribution by repetitive measurements, it may be relatively large with few degrees of freedom; thus causing the combined standard uncertainty to be too small to adequately represent the true uncertainty of the measurement. This may occur, for example, in calculation of a radiated immunity uncertainty estimate. While this is a "second order" effect, this appendix should help in understanding when consideration of degrees of freedom is required.

The degrees of freedom associated with a contributing uncertainty $u_i(y)$ are ν_i, and the effective degrees of freedom associated with the combined standard uncertainty $u_c(y)$ are given by Equation (C1).

$$\nu_{eff} = \frac{u_c^4}{\frac{u_1^4}{\nu_1} + \frac{u_2^4}{\nu_2} + \frac{u_3^4}{\nu_3} + \cdots + \frac{u_m^4}{\nu_m}} \quad \text{(C1)}$$

The degrees of freedom for Type B evaluated contributing uncertainties are assumed to be ∞. If all ν_i in Equation (C1) are ∞, ν_{eff} is then ∞ and $k_p = k$.

When one or more contributing uncertainties are found by Equation (1), the combined standard uncertainty multiplied by k may not give the needed probability (p) of coverage. The coverage factor k needs to be calculated as k_p in accordance with Appendix B of TN 1297 [8]. Following is a brief discussion of the method.

If one contributor is normal from repeated measurements and all others are Type-B (for example three others), rewriting Equation (C1) gives:

$$\nu_{eff} = \frac{u_c^4}{\frac{u_1^4}{\nu_1} + \frac{u_2^4}{\infty} + \frac{u_3^4}{\infty} + \frac{u_m^4}{\infty}} = \frac{u_c^4}{\frac{u_1^4}{\nu_1}} = \nu_1\left(\frac{u_c}{u_1}\right)^4 \quad \text{(C2)}$$

$\nu_1 \geq 1$, [this is always true, because $\nu = n-1$ and always $n \geq 3$] then,

$$\nu_{eff} \geq \left(\frac{u_c}{u_1}\right)^4 \quad \text{(C3)}$$

If $\frac{u_c}{u_1} \geq 3$, then $\nu_{eff} \geq 3^4 \geq 81$, and $k_p = 2$ is acceptable for 95% confidence. See the following tabulation for p = 95.45%, which comes from Table B.1 of TN 1297 [8], and is based on student's-t distribution.

[1] All numbers in square brackets refer to documents in the reference section at the end. They are listed in the order in which they are referenced in the text.
[2] The normal distribution is defined later in the article.
[3] This is a condition that seldom occurs in EMC measurements.

TABLE C.1

ν_{eff}	1	2	3	4	5	6	7	8	10	20	50	∞
k_p	13.97	4.53	3.31	2.87	2.65	2.52	2.43	2.37	2.28	2.13	2.05	2.00

Donald Heirman is President of Don HEIRMAN Consultants, a training and educational EMC consultation corporation. Previously he was with Bell Laboratories for over 30 years in many EMC roles including Manager of Lucent Technologies (Bell Labs) Global Product Compliance Laboratory where he was in charge of the Corporation's major EMC and regulatory test facility. He chairs, or is a principal contributor to, national and international EMC standards organizations including ANSI ASC C63 and the Special International Committee on Radio Interference (CISPR) of the International Electrotechnical Commission (IEC) that develop new emission and immunity instrumentation specifications and measurement techniques. Mr. Heirman is a Fellow of the IEEE, a member of its EMC Society Board of Directors (and its Vice President for Standards), chair of the Society's Electromagnetic Compatibility Measurement Committee, and has authored and presented internationally numerous papers, tutorials, and seminars/workshops on EMC subjects. He is also the President-elect of the IEEE Standards Association, immediate past chair of the IEEE Standards Association Standards Board, and is the immediate past President of the National Cooperation for Laboratory Accreditation (NACLA). He is the vice-chairman of the American National Standards Institute Accredited Standards Committee C63 and chairs its Subcommittee One on EMC Techniques and Developments. Subcommittee One prepares guidelines or standards for EMC measurements, test site qualifications, antenna calibrations, automated measurements, and emission and immunity limit setting. Mr. Heirman is a technical expert for CISPR Subcommittees A (radio interference measurements and statistical techniques) and I (formerly Subcommittees E and G) (information technology, radio receivers and multimedia) and is a member of the CISPR Steering Committee. He is also the Subcommittee A chairman responsible for CISPR 16 which is the basic horizontal standard for measurement instrumentation and measurement techniques for all the CISPR product committees. He is a member of the IEC's Advisory Committee on EMC (ACEC). He is also group manager for electromagnetics for the U.S. National Committee Executive Committee (now called the Technical Management Committee) of the IEC responsible for facilitating primarily the CISPR and TC77 (immunity) US participation and Chair of its Coordinating Committee on EMC. Mr. Heirman is also an adjunct professor/senior research scientist at the University of Oklahoma and is the Associate Director for Wireless EMC at the University's Center for the Study of Wireless EMC. He is a retired Commander in the US Navy Reserves and he is a listed in multiple Who's Who publications.

Edwin L. (Ed) Bronaugh is a Life Fellow of the IEEE, an Honorary Life Member of the EMC Society, and a Life Member of the IEEE Standards Association. He has often served on the EMC Society Board of Directors, and is a past president of the Society. He is also a distinguished lecturer on EMC topics. He is a member of the EMC Standards Committee and is an Emeritus Member of ANSI-Accredited Standards Committee C63. He is a member of the US Technical Advisory Groups for CISPR, CISPR/A and CISPR/I. The EMC Society awarded him the Certificate of Appreciation in 1979, the Certificate of Achievement in 1983, the Certificate of Acknowledgment in 1985, the Richard R. Stoddart Award in 1985, the Laurence G. Cumming Award and the Standards Medallion in 1992, a Standards Development Certificate in 1993, and the IEEE Third Millennium Medal in 2000. He has authored a book on EMI measurements and authored over 150 papers for professional meetings and publications. He is a senior member of the National Association of Radio and Telecommunications Engineers (Certified EMC Engineer). He is listed in Who's Who in America, Who's Who in the World, Who's Who in Science and Engineering, Who's Who in the South and Southwest, and Men of Achievement. Mr. Bronaugh is Principal of EdB™ EMC Consultants, an independent EMC consulting firm. Previously, he was Lead Engineer for Hardware Design Assurance at Siemens Communication Devices, Austin, Texas, Vice President for Engineering at the Electro-Mechanics Company, Technical Director of Electro-Metrics, and Manager of EMC Research at Southwest Research Institute.

Magnetic Light Technology—Illumination for the 21st Century and Beyond

Steve Vetorino, Geoffrey Wilson, and Russell Sibell

Background

With the development of rare-earth magnets towards the end of the 20th century, generators capable of converting mechanical to electrical energy reached astounding efficiencies. Presently, efficiencies of 85% are not uncommon. Also, the need for memory back up in personal computers and the need for energy efficient, maintenance free illumination led to remarkable advancements in high-energy capacitors and solid state light emitting devices. As these technologies developed, ways to integrate them were explored by a small company in Colorado. Ultimately, Applied Innovative Technologies, Inc. produced the world's first commercially available flashlight that used no batteries or incandescent bulbs and would work even after years of abuse and neglect.

The NightStar flashlight integrates a linear generator with state-of-the-art electronics. By shaking NightStar, kinetic energy is transformed into electrical energy by means of repeatedly passing a high field strength magnet through a coil of wire. The electrical energy generated is rectified from a bipolar current impulse to direct current. Rather than batteries, a capacitor stores the energy produced by the generator. The capacitor, though incapable of powering inefficient incandescent lamps for more than a few seconds, can power the LED for more than 20 minutes on a single charge. The light output from the LED is projected into a uniform beam by a specially designed acrylic lens and reflector. To ensure operation under all conditions, NightStar's components are contained within a waterproof, polycarbonate housing.

At the heart of the flashlight are high-strength magnets. The ferromagnets used in NightStar are an anisotropic sintered ceramic containing neodymium, iron and boron (NdFeB). The anisotropic nature of the material (meaning that it has properties that differ according to the direction of the measurement) is due to the tetragonal crystalline structure of the NdFeB molecule. The magnetic dipole associated with each crystal lattice site aligns itself along a well-defined axis within the bulk material. As a consequence of its molecular magnetic structure, the material is remarkable in two ways. First, it possesses a high-density magnetic field because of the alignment uniformity of the magnetic dipoles, and second, it will hold this field for an extremely long time even when orientated for repulsion with another magnet or subjected to relatively high temperatures and shock. Remarkably, the field strength at the core of the charging magnet is approximately 45 million gauss. Along the surface of the magnet the field is approximately 8 thousand gauss and at 1 foot the field is still an astounding 300 gauss.

NightStar contains four neodymium rare earth magnets, one that is free to travel within a tube that runs nearly the length of the flashlight, one fixed at each end of the tube, and one that activates the internal reed switch. The fixed magnets are oriented in the same direction while the mobile magnet is oriented oppositely. This creates a repulsion that traps the mobile magnet (hereafter referred to as the charging magnet) part way between the fixed magnets. When NightStar is shaken, the magnetic repulsion recoil system smoothly rebounds the charging magnet without loss in energy. Consequently, the loss of energy due to friction is extremely small and is only the result of the cylindrically shaped nickel-plated charging magnet sliding along polished rails. Kinetic energy is therefore efficiently converted into electrical energy with almost no wear and tear on system components due to friction. Because of this, and due to the fact that NdFeB magnets can withstand demagnetization, lasting performance is obtained.

In its broadest definition, magnetism is the force exerted between moving charges due to their motion. This is distinct from the *electrostatic force*, which exists between charges regardless of their motion. Magnetic force can be demonstrated by passing electrical current through neighboring coils of wire and observing their mutual attraction or repulsion. Unlike coils, the permanent or ferromagnets used in NightStar need no source of current. Current is produced by the electrons orbiting around the nucleus of each atom in the magnet. These tiny electrical currents occur in all matter, and yet most materials are not magnetic because the currents produced by pairs of electrons oppose one another and magnetism is canceled out. In a ferromagnet, however, nearly all the uncancelled electron currents are aligned and working together to produce a strong magnetic force. Ferromagnets are directional. If two ferromagnets are placed end to end, oriented so that their electron orbits are in the same direction, they will attract each other. If the magnets are oriented so that their electron orbits oppose, they will repel each other. Attraction and repulsion both strengthen with decreasing distance between the magnets. For any ferromagnetic material, the field strength drops off approximately as the inverse cube of the distance.

NightStar exploits the magnetic force between moving electrons in yet another way. A coil of copper wire wound about the midpoint of the tube transforms the mechanical energy of the moving magnet into electrical energy. To better understand this process, it is convenient to imagine the magnet as fixed, and the coil moving past it, as shown in Figure 1. The moving charged particles in each copper atom in the coil all respond as they pass the magnet. However, all but one of the charges are embedded in the material and are unable to break free of their bonds. The exception is the single free electron per copper atom, which is able to move about in the material. Initially we will assume that each free electron is stationary within the wire, which means it is moving parallel but displaced to the side of the magnet axis. As the free electron approaches the magnet, it experiences a force that is perpendicular both to its direction of motion and to a line drawn through and perpendicular to both the direction of motion and magnetic axis. This force happens to be along the direction of the coil wire, and the free electron will begin moving along the wire, along with a huge number of free electrons from other atoms. This mass motion peaks as the coil passes the end of the magnet, where the magnetic field is most perpendicular to the coil. As the coil passes the center of the magnet, the motion slows to a halt and then reverses direction, peaks in the opposite direction and then slows to a halt again as the coil recedes.

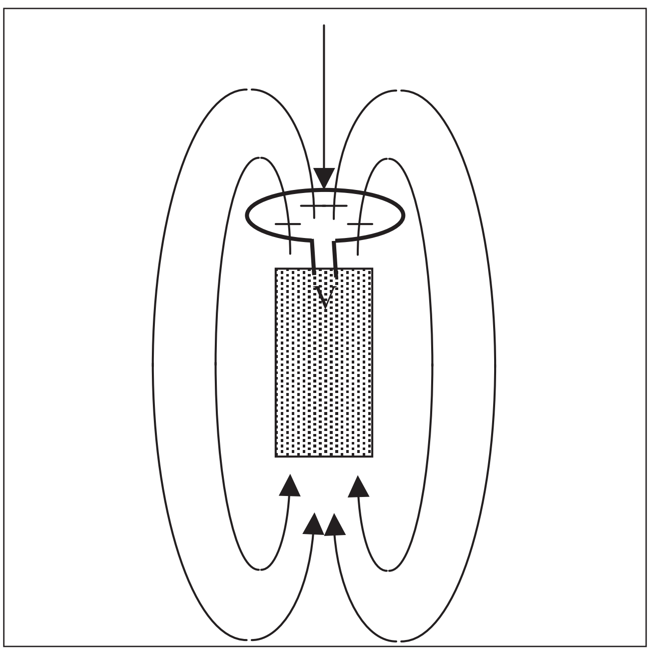

Figure 1.

This microscopic picture of magnetomotive induction had to wait for the discovery of sub-atomic particles. Historically, magnetomotive induction was first described in macroscopic terms, following the experiments of Faraday and others in the early nineteenth century. An idealized experiment is shown in Figure 1. When a single loop of wire is passed over a magnet, the induced voltage V is proportional to how fast the number of field lines (arrows going from the top to the bottom magnet pole) surrounded by the loop changes in time. Mathematically, this is:

$$V = -\frac{d\Phi}{dt} \text{ where } \Phi \equiv \oint dS\,\hat{n} \cdot \vec{B}$$

where Φ is the "flux", or number of field lines going through the coil, B is the magnetic field vector, and S is the surface through which the field is passing. As the coil moves down over the magnet, the flux increases until the coil reaches the midpoint, and then begins to decrease. The time derivative of the flux, and therefore the voltage, is maximum when the coil is near either end of the magnet, and zero at the midpoint.

Of course, a single loop of wire produces a feeble voltage, and standard practice is to loop many winds into a coil. A central problem in magnetic design is how many winds are needed in the coil. There are actually two issues—how long to make the coil, and how thick the coil wire should be. If we imagine starting with one wind and adding one at a time along the axis, we would initially find that each additional wind adds an increment of voltage equal to that of the original wind. As long as the coil is short compared to the magnet, all the winds see the same change in flux at the same time, the induced voltages add, and the total voltage is proportional to the number of loops. Eventually, though, when the coil becomes longer than the magnet, winds on one end see a decrease in the flux at the same time winds at the other end see an increase as the coil passes the magnet, so that their voltages cancel. At this point adding more winds to lengthen the coil becomes ineffective and still more length becomes detrimental. We have found the optimum total travel distance of the magnet should be 5 times the length of the magnet for the field lines to effectively clear the coil. This geometry produces an ideal single bipolar pulse of energy for each pass of the magnet as shown in Figure 2.

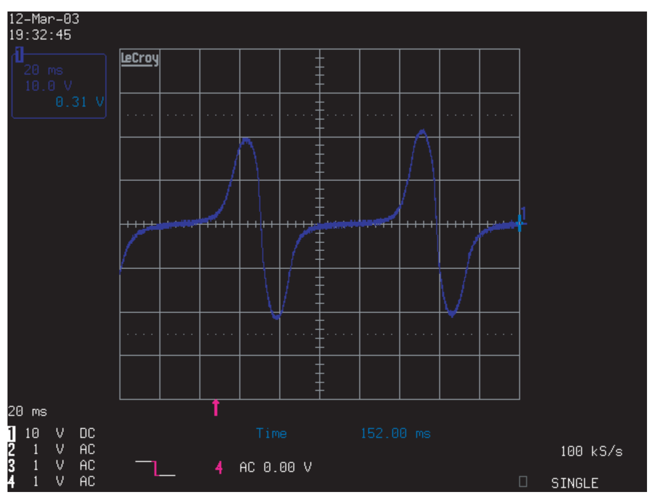

Figure 2.

With regards to the wire diameter, large diameter wire allows for higher current with less resistance but reduces the total number of winds that can fit in the allowed coil volume and therefore reduces the peak voltage. Small diameter wire has lower current and higher resistance but allows for more winds and higher peak voltage. The optimum wire was found to be 30-gauge magnet wire, which most effectively couples kinetic to electrical energy and minimizes the effort needed to recharge the capacitor.

The electrical current produced by the ferromagnet moving through the coil goes in one direction as the magnet approaches the coil, and the other as the magnet recedes from the coil. This so-called alternating current is not the most useful form for either storage or conversion to light. NightStar uses four diodes as a full-wave bridge rectifier to convert alternating current to the more useful (for our purposes) one-way form, called direct current.

A diode is formed when an n-type and a p-type semiconductor are brought into contact to form a "junction". An n-type semiconductor is similar to copper in that some atoms have a loosely-bound electron that can easily be freed to flow through the material, and thus contribute to an electrical current. P-type semiconductors have atoms with too few tightly-bound electrons, which causes them to steal an electron from one of their neighbors. Atoms on the p-type side pull electrons from the n-type side across the junction, to fill their vacancies. The effect of this transfer of electrons is that the n-type material loses electrons and becomes positively charged, making it increasingly difficult for more electrons to leave. The tendency of electrons to stay quickly balances the tendency to leave, and the exodus ceases. For electrons to continue to cross the junction from the n- to the p-type side, the dwindling supply of electrons in the n-type material must be replenished thereby reducing its positive charge. Simultaneously, excess electrons in the p-type material must be drained away, thereby reducing its negative charge. We can accomplish both objectives by connecting a battery to the diode, negative terminal to n-type and positive terminal to p-type. In so doing, a current of electrons will then flow indefinitely in the circuit, in the direction of n-type to p-type material. If, however, the battery is connected backwards, the n-type material becomes even more positively charged, so that it pulls back some of the electrons that formerly crossed the junction to fill vacancies in the p-type material. This retraction of electrons is quickly balanced by the increasing demand to fill p-type vacancies, and the brief flow of electrons stops. If the reverse voltage is increased, another brief increment of charge is transferred, but no permanent current is established. In this way, the diode acts as a one-way street for electrons, or as a check valve acts in a plumbing system.

Referring to Figure 3, when the magnet approaches the coil, the current path of electrons will flow as shown in red.

When the magnet passes the coil and recedes, electrons will flow as shown in Figure 4. Therefore, no matter which direction the current flows in the coil, it flows in one direction in the load. This is called rectification.

Once the current has been rectified, the energy associated with each pulse can be stored in a capacitor. A capacitor consists of two flat metal plates with a thin layer of insulator between them. When connected to a battery or other charging source (in our case a linear generator), electrons leave the negative terminal and pile onto one of the capacitor plates. As they build up, they repel electrons on the other plate. The electrons on the far plate travel to the positive terminal of the charging source. Under these conditions no single electron travels through the entire circuit. This situation is temporary because the growing imbalance of electrons between the plates increasingly inhibits further current, until eventually it dwindles to nothing. At this point, the capacitor is said to be "charged". Its plates have a voltage difference that

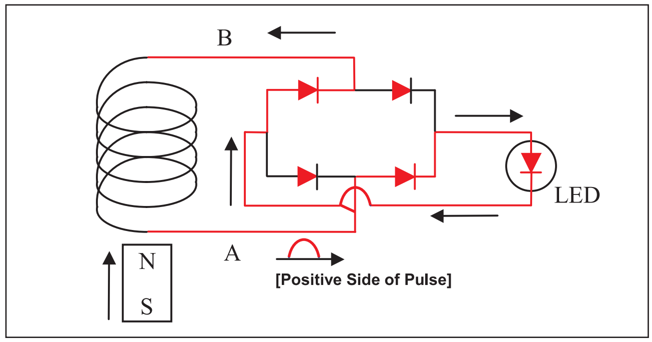

Figure 3.

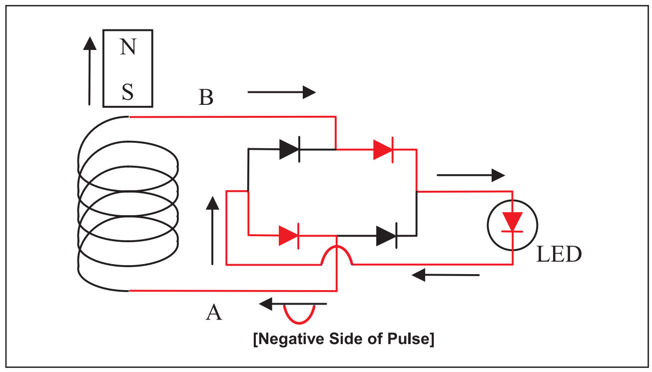

Figure 4.

opposes the voltage source and prevents further charging. The ratio of the stored charge Q to the voltage V is the capacitance C

$$C = Q/V$$

If a load suddenly replaces the charging source, electrons will take advantage of the newly available current path by flowing from the crowded plate, through the load, and onto the depleted plate. This current will continue until the electrons are equally distributed on the two plates, and the voltage difference is zero. This temporary current dissipates an amount of energy that turns out to be independent of the nature of the load, and given by the equation:

$$E = 1/2CV^2$$

The capacitor used in NightStar is a 1-Farad, 5.5V, double layer gold capacitor, which stores up to 15 joules of energy. The capacitor can hold a charge for several months and can be recharged several hundred thousand times. In addition, it contains no corrosive chemicals and will power the LED even when subjected to extreme hot and cold temperatures.

Another important function of the semiconductor diode is to radiate light. While all diodes rectify current, not all radiate. A small bundle of light called a photon may be generated when an electron and a hole collide and annihilate each other. Whether or not this happens depends on the details of the collision.

Prior to their collision, the electron and hole each have an energy and a momentum associated with their motion. Momentum is a measure of how much effort it takes to stop a moving object, which is proportional to both the mass and the speed of the object. Momentum has a second, equally important aspect, directionality. It points along the direction of motion. Indeed, momentum is usefully represented by an arrow pointing in the direction of motion, whose length is given by mass times speed. Energy is the other quantity associated with the motion of an object. It has no directionality, and is proportional both to the mass, and to the speed times itself, or the speed squared.

Electron and hole annihilation typically produces either a photon, or a small bundle of sound called a phonon. In either case, the product must have the same total momentum and the same total energy as the free electron and hole. In the annihilation, the free electron is now bound and so it no longer exists as a free electron, and the hole is filled by the bound electron and so it too no longer exists. Both the free electron and hole give up their momentum and energy in the process. Whereas a phonon (sound) has quite a bit of both energy and momentum, a photon (light) has considerable energy but almost no momentum. Therefore, a collision between an electron and hole that don't have equal and opposite momenta always produces a phonon to carry the net momentum away. A photon can result only when the electron and hole have nearly equal and opposite momenta. It happens that in semiconductors used in common diode rectifiers, such as silicon and germanium, electron and hole momenta have differing magnitudes (mass times speed) that cannot cancel each other, and so their collisions do not produce light. Such collisions are called nonradiative recombinations. In certain, more costly semiconductors such as gallium arsenide, electron and hole momenta can cancel, so that a photon may be emitted, an event called a radiative recombination.

Light-emitting diodes (LEDs) are based on radiative recombination. The first LEDs were made of gallium arsenide, a material that emits infrared light. Gallium arsenide is an example of a III-V (three-five) compound semiconductor, inasmuch as gallium is a member of the III family of chemical elements, and arsenic is a member of the V family. Investigators realized that other members of the III family could be substituted for gallium and others of the V family for arsenic, so that visible colors could be radiated. Specifically, adding lighter elements of each group (aluminum for group III, and phosphorus or nitrogen for group V) would give shorter wavelengths. First, red LEDs were achieved by replacing some gallium with aluminum. Later, yellow and green LEDs were made by replacing some arsenic with phosphorus.

Blue LEDs have long been eagerly sought. They are the crucial third component of RGB (red-green-blue) LED displays. RGB devices can catalyze chemical reactions in printing and photolithography that longer wavelengths cannot. They can also achieve greater densities in optical data storage such as the DVD-ROM format. In addition, they can excite red and green fluorescence in special phosphors to mix with remaining blue to create white light. However, they defied the efforts of many researchers until a group at the Nichia Corporation in Japan began to succeed with gallium nitride LEDs in the mid-90s. The NightStar flashlight contains an LED that converts 60 mW of electrical power into 18 mW of white light, a feat that would have been considered miraculous in the mid 1990's. It should be noted that white light diodes are less efficient than green and red diodes because of an internal conversion loss. As high-energy 440 nanometer photons pass through a phosphor layer they generate photons of all colors. The conversion of blue photons into other colors however, is only 50% efficient. The product of the initial blue photon generation efficiency and the white light conversion efficiency gives an overall device efficiency of 30% (60% × 50%).

The light collection and imaging system contains two key optical elements, a reflector and lens. The reflector directs side emission light forward and the lens produces a uniform and nearly collimated beam of light. The reflector has a conical profile. When placed over the LED it redirects side band light in a forward direction. A bright shaped oval of light at the apex of an LED's plastic housing is produced by total internal reflection inside the plastic. The light emitted from this bright spot exits the LED nearly perpendicular to the normal forward going light. The side band light has between 10 and 20% of the light output power of the forward going light. If no reflector is used, this light is wasted. A reflector with a 70-degree cone angle redirects the side band light forward through the lens. The axial position of the diode inside the reflector determines how much light is collected and where it will overlap the forward going light. Experimentally it was found that the conical reflecting surface should intersect the LED 0.04 inches below the center of the hemispherical dome of the LED housing in order to optimize light gathering and beam overlap. The reflector, as described above, will place side band light on top of the forward going light approximately 10 feet in front of the lens.

A great deal of consideration was given to the switch. In the end, a magnetically activated reed switch was selected. This design feature has several advantages over conventional mechanical switches. The most significant advantage is reliability. The sliding plastic switch holding a magnet on the outside of the light can't corrode or wear out and the reed switch mounted on the circuit board inside the flashlight is rated at over 1 million cycles. In comparison, mechanical push button or toggle switches have contacts that corrode and springs that fatigue after a relatively small number of on/off cycles. A key advantage to NightStar's switch design is that it doesn't require a watertight seal; the magnet on the outside is able to activate the reed switch through the plastic housing. Finally, because the electrical circuit is not exposed to the outside world (as with a typical mechanical switch) there is no possibility of igniting combustible materials.

Finally, NightStar's plastic housing proved to be as critical to the operation of the light as the cutting edge electronics. A metallic housing would render the generator useless by preventing the charging magnet from moving effectively through the coil. This is due to free electron eddy currents being set up in the metal housing when the charging magnet travels through the barrel. Consequently, magnetic fields generated by the eddy currents in the housing oppose the magnetic field of the charging magnet. The faster the charging magnet tries to move, the stronger the opposing fields will be in the housing, effectively "braking" the magnet's motion. Therefore, the charging magnet would never pass through the coil with enough speed to charge the capacitor. The plastic housing is superior to a metal housing in several other ways as well. The material and manufacturing costs of plastic are far less expensive than aluminum (aluminum is a likely choice for a metal housing). Additionally, NightStar's plastic housing will never rust or oxidize and weighs less then an aluminum housing that would provide the same amount of crush resistance. The polycarbonate plastic used in NightStar was chosen for two reasons. First, it is difficult to break even at cold temperatures, and second, it is unaffected by salt water, mild acids, alcohol, ammonia based cleaners and petroleum products such as diesel fuel, motor oil and grease.

The Sum of All the Parts ... System Integration

The circuit diagram in Figure 5 shows the key electronic and magnetic components discussed thus far. In order to study the interplay of all the components and the flow of energy through the system, we will begin with the coil and magnet. Referring to $V = -\frac{d\Phi}{dt}$ where $\Phi \equiv \oint dS\,\hat{n} \cdot \vec{B}$ and the discussion regarding numerous coil windings, the voltage generated by the magnet moving through the coil can be calculated by the equation:

$$V = V_{Peak}\,(\sin(\omega t)) \text{ where } V_{Peak} = (N)(B)(A)(\omega) \text{ and } \omega = \pi/T$$

In this equation, V_{Peak} is the maximum peak voltage of the sine wave pulse. The number of coil windings is N, B is the magnetic field strength of the magnet (measured in Tesla), A is the cross sectional area of the coil (measured in meters squared), and T is the pulse duration (measured in seconds). For NightStar, N = 1472, B = 0.54, A = 0.0006 and at 3 shakes per second, T = 0.06 seconds. The theoretical peak voltage is nearly 25 volts. Experimentally the peak voltage was measured to be approximately 22 volts, as shown in Figure 3.

The resistance of the coil is given by the equation:

$$R = \frac{(z)(\rho)}{a}$$

where z is the total length of wire in the coil, ρ is the resistivity of the wire (measured in ohms * meters) and a is the cross sectional area of the wire. For the 30 gauge copper wire used in NightStar, z = 137 meters, $\rho = 1.7 \times 10\exp(-8)$, and $a = 5 \times 10\exp(-8)\ m^2$, which gives a total coil resistance of about 45 ohms. Experimentally the coil resistance was found to be 43 ohms.

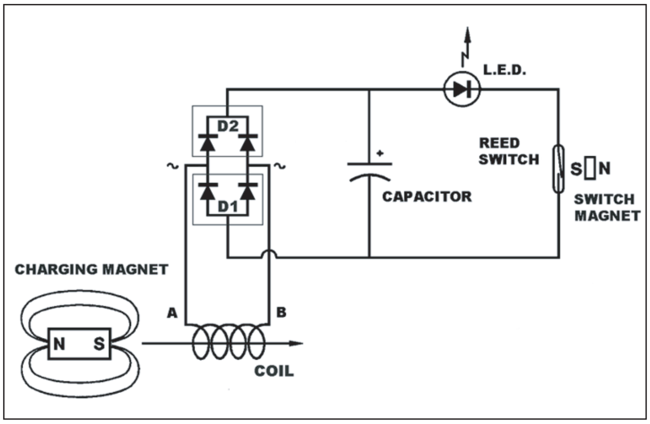

Figure 5.

Once the voltage and resistance of the circuit are known, an equation for the power as a function of time can be derived:

$$P = \frac{V^2}{R} = 21^2\frac{(\sin^2(\omega t))}{R_{inductor}} = 441\,\frac{(\sin^2(\pi/T)\,t)}{43}$$

$$= 10.25\,(\sin^2(\pi/T)\,t) = 10.52\,(\sin^2 52t)$$

The energy per sine wave pulse is then the integral of the power from 0 to 0.06 seconds:

$$E = \int_0^{.06} P\,dt = \int_0^{.06} 10.25\,(\sin^2 52t)\,dt$$

$$= 10.25\left[\frac{t}{2} - \frac{\sin(2)(52t)}{(4)(52)}\right]_0^{.06}$$

$$= 10.25\left[\frac{.06}{2} - \frac{\sin(104)(.06)}{208} - \frac{\sin(104)(0)}{208}\right]$$

$$= 10.25\,[.03 - .0005] = 0.30 \text{ joules}$$

By assuming that the circuit is about 50% efficient (a reasonable value for electrical circuits of this kind), then approximately 0.15 joules are dumped or stored into the capacitor with each shake.

In order to calculate the coupling efficiency from kinetic to electrical energy, we must determine the speed of the magnet as it moves through the coil. The magnet travels a distance equal to 4 times its length in 0.06 seconds. This corresponds to a maximum speed of approximately 4 meters per second when you take into account acceleration at the ends of travel. The kinetic energy of the magnet is given by the expression:

$$E = 1/2mv^2$$

where m is the mass of the magnet (0.06 kg) and v is its velocity. Replacing m and v with their appropriate values gives a kinetic energy of 0.48 joules. This is the total kinetic energy of the magnet. Only part of this kinetic energy is extracted since the magnet does not slow to zero velocity as it passes through the coils. The coupling efficiency from kinetic to electric energy is therefore 62% (0.30/0.48). This conversion efficiency corresponds to the magnet slowing by about 39% as it passes through the coils. It should also be noted that the coupling ratio changes as a function of the charge in the capacitor. When the capacitor is drained of energy the conversion from kinetic to electric energy is higher. The slowing down of the magnet as it passes through the coil is evidence of this. As the capacitor becomes fully charged, less and less energy is extracted with each pass of the magnet through the coil. As a result, NightStar becomes easier to shake.

The two high-speed switching diodes (designated D1 and D2) when wired as shown in Figure 5 act as a full-wave bridge rectifier. Figures 6 through 8 show the voltage measured across the capacitor terminals on the circuit board. After rectification, energy generated by the magnet passing through the coil appears as positive going pulses. With each shake the DC voltage level of the capacitor increases.

When the reed switch is closed, energy in the capacitor (designated C1) powers the Light Emitting Diode (LED). The total energy that can be stored in the capacitor is about 15 joules ($E = \frac{1}{2}CV^2$) In NightStar, the LED operates from 5.5 volts, the maximum voltage across the capacitor, to approximately 2.8

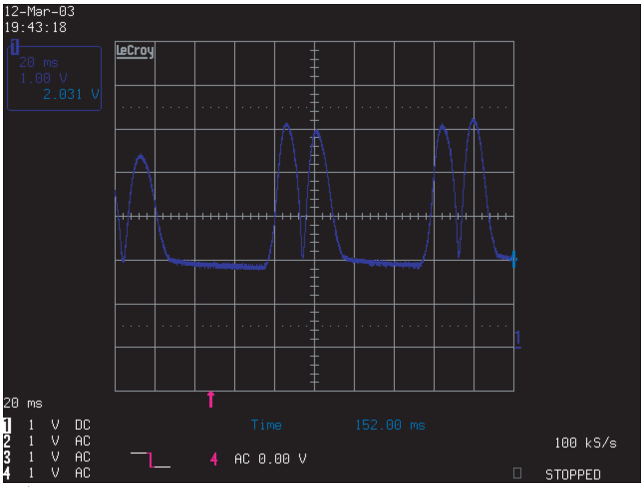

Figure 6.

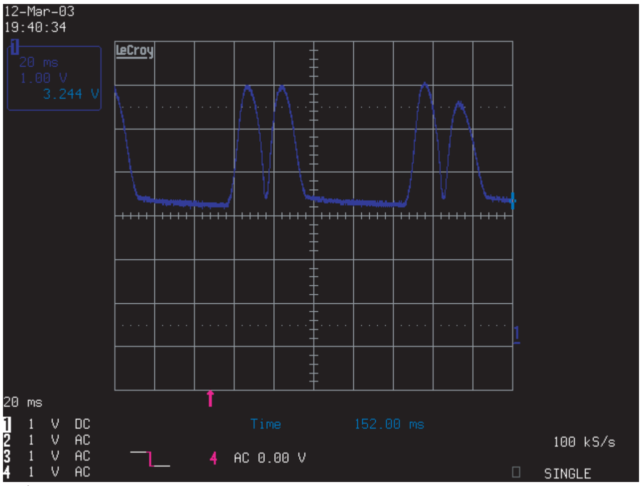

Figure 7.

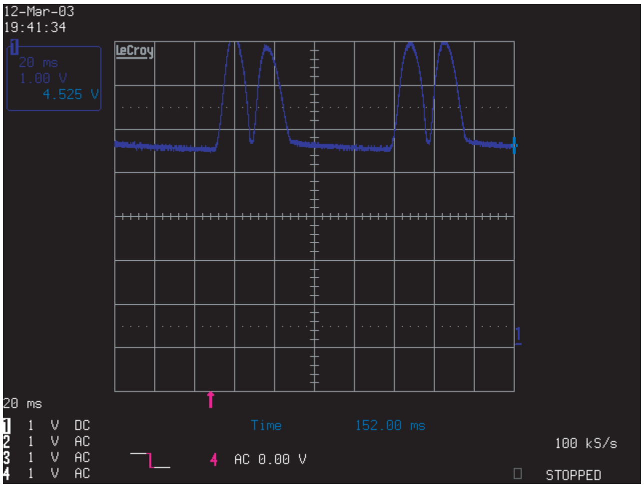

Figure 8.

volts, which is the minimum turn on voltage for the LED. Consequently, the energy extracted from the capacitor by the LED is approximately 12 joules ($\frac{1}{2}C[(5.5)^2 + (2.8)^2]$). It will therefore take about 80 shakes to recharge the capacitor (12 joules/0.15 joules/shake). It should be pointed out that the capacitor leaks off energy at a rate of approximately 0.13 joules per day, which means that it will take nearly 3 months to completely discharge. As a result, if NightStar is left unused for an extended period of time, it will take about 100 shakes to fully re-energize it (15 joules/ 0.15 joules/shake).

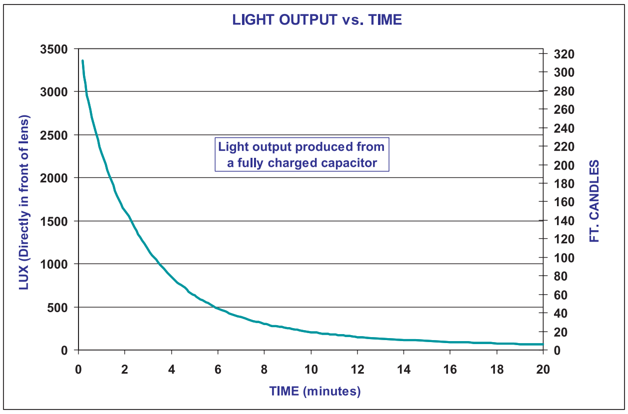

Figure 9.

The LED used in NightStar is a 3-volt, 20 to 30 mA solid-state device with an efficiency of 30%. Initially, and on a full capacitor charge, NightStar produces nearly 0.02 watts of visible light with a corresponding luminous flux and intensity of 3360 Lux and 312 ft-candles, respectively. Due to the discharge characteristics of the capacitor this drops off and reaches a relatively stable state after 4 to 5 minutes, as shown in Figure 9.

Testing & Beyond

In order to quantify NightStar's intrinsic and operational characteristics it was subjected to a wide range of tests conducted by independent laboratories across the country. NightStar is now certified safe for use in explosive environments filled with volatile substances such as acetylene, hydrogen, natural gas, and aviation fuel. NightStar can also withstand chemicals such as phosphoric acid, drain cleaner, salt water, bleach and diesel fuel. Even when subjected to high impact drop tests and exposed to extreme temperatures, NightStar continued to operate. NightStar even survived deep-water submersion to a depth of over 2200-ft. and passed the requirements of the ASTM marine safety standard.

Now, after more than six years, NightStar has triggered a worldwide interest in magnetic light technology. Presently, there are at least four other companies producing flashlights based on NightStar's patented design. Without a doubt, the magnetic force flashlight is gaining acceptance and recognition and may eventually become a standard piece of emergency equipment. In the larger picture, the integration of high strength magnets and capacitor energy storage may one day be used to reliably power a wide range of electronics.

To learn more about NightStar, please visit our web site at www.nightstar1.com

Contact: svetorino@nightstar1.com

Contributing Authors:
Steve Vetorino, Co-Founder of Applied Innovative Technologies, Inc.,
Geoffrey Wilson Ph.D.,
Russell Sibell

Russell E. Sibell *received his Bachelor of Science in Physics and Chemistry from North Dakota State University. In 1982, Mr. Sibell was commissioned as an Air Force Officer and worked on the Airborne Laser Laboratory to its completion. Mr. Sibell also worked for Spectra Physics as a Quanta-Ray Service Engineer, and for Mission Research Corporation as a Laser Engineer. Mr. Sibell joined Coherent Technologies in 1996. As a Senior Research Laser Engineer, his primary responsibilities include optical design in telescopes, beam imaging systems, polarization optics, and testing and construction relating to the development of lidar systems. He is also currently pursuing study in nuclear energy technology.*

Steven R. Vetorino *received his Bachelor of Science in Physics from Colorado State University. In 1984, Mr. Vetorino began working with Spectra Physics as a Field Engineer. There he specialized in the installation of custom ultra short pulse YAG-dye laser systems. In 1990, he joined Coherent Technologies, Inc. As a Senior Research Engineer at CTI, he served as a technical lead on programs developing state of the art laser radar systems for use in atmospheric profiling and bio-chem detection. In 1997, Mr. Vetorino Co-Founded Applied Innovative Technologies, Inc. His diverse responsibilities at AIT include: evaluation of new technologies; prototype design and development; establishing and optimizing product quality control procedures; management of product testing and certification; management of marketing efforts, and technical customer support.*

Geoffrey Wilson *has been in laser and optics research for eighteen years. His postgraduate work involved methane leak detection using differential absorption lidar, and the dynamics of coupled diode lasers. Since receiving a Ph.D. in applied physics, he has led projects in experimental quantum optics, all-optical multiple read/write data storage, remote vibrometry using coherent laser radar (CLR), aircraft CLR for winds-aloft measurements, and the laser induced fluorescence detection of airborne pathogens. He has about thirty journal papers and conference presentations, and several patents. He is presently ramping up a second career as a technical author.* **EMC**

EMC Fest 2004

A One-Day Colloquium and Exhibition on: EMC Coupling Mechanisms and Diagnostic Techniques

Thursday, May 6, 2004 Dearborn Inn Dearborn, Michigan

Featuring Industry Renowned Speaker: **Tom Van Doren** of the University of Missouri-Rolla

For further information:
Kimball Williams, Chairman: Ph: 248-427-5325, e-mail: *k.williams@ieee.org*
Janet O'Neil, Vice-Chair Exhibits: Ph: 425-868-2558, e-mail: *j.n.oneil@ieee.org*

Home page: ***http://www.emcsociety.org/***
Register On-Line!

Sponsored by the Southeastern Michigan Chapter of the IEEE EMC Society.